Temporal variation of sound speed in ocean: a comparison between GPS/acoustic and *in situ* measurements

Motoyuki Kido, Yukihito Osada, and Hiromi Fujimoto

RCPEV, Graduate School of Science, Tohoku Univ., Aoba-ku, Sendai 980-8578, Japan

(Received September 14, 2007; Revised November 30, 2007; Accepted December 19, 2007; Online published March 3, 2008)

The GPS/acoustic technique applied to seafloor geodesy intrinsically measures integrated sound speed along a trajectory of an acoustic signal as well as the position of a seafloor transponder array. We present here a generalized expression of sound speed variation in terms of a traveltime residual normalized to the vertical component. With this expression, residual traveltimes to any seafloor transponders will have a same value regardless of their depths and slant angles. This is valid even for the case having horizontal gradient in sound speed structure; the gradient affects only on positioning of a transponder array and not on the estimate of sound speed just beneath the observation point. We monitored temporal variation of this quantity through a GPS/acoustic survey and compared it with *in situ* expendable bathythermograph (XBT) measurements periodically carried out during the survey. We found that the relative change of the two independent measurements are in good agreement within 5% of the typical amplitude of temporal variation.

Key words: GPS/acoustic technique, seafloor geodesy, sound speed, XBT.

1. Introduction

A combined technique using the Global Positioning System and underwater acoustic ranging (GPS/acoustic) has now been put to practical use in seafloor geodesy to provide crucial observations of seafloor deformation where land-based GPS networks are hardly adaptable (Spiess *et al*., 1998). As the application of the GPS/acoustic technique to monitor steady crustal movement near the subduction zones, strong interplate coupling between the subducted slab and overlaying plate is observed along the Peru-Chile trench (Gagnon *et al*., 2005) and the Japan trench (Fujita *et al*., 2006). For mid-ocean ridges, Chadwell and Spiess (2007) found the evidence of an intraplate local extension zone near the Juan de Fuca ridge based on the facts of their repeated GPS/acoustic observation of steady spreading at 25 km away from the ridge crest and of no significant spreading across the 1 km-wide axial valley (Chadwell *et al*., 1999; Chadwick and Stapp, 2002). The GPS/acoustic technique is also applicable to detect episodic events beneath the ocean. Coseismic displacements of seafloor were detected for the 2004 Off Kii-Peninsula earthquake at Kumano-nada along the Nankai trough (Kido *et al*., 2006; Tadokoro *et al*., 2006) and for the 2005 Off Miyagi Prefecture earthquake along the Japan trench (Matsumoto *et al*., 2006).

As Spiess (1985) made a proposition more than twenty years ago, the GPS/acoustic technique consists of two components: one is monitoring the position of an acoustic transducer at the sea-surface through the kinematic GPS method and the other is acoustic ranging between the transducer and three or four acoustic transponders placed on the seafloor. The acoustic ranging is directly affected by the sound speed variation along the trajectory of sound waves. Fortunately, most part of spatio-temporal sound speed variation is confined in shallow water column and is well approximated by time-depending horizontally stratified structure at least within a horizontal scale bounded to the shallower trajectory. In this case the net effect of sound speed variation on traveltimes to all the transponders at a certain time is described by a scalar quantity and can be simultaneously solved with the positions of the transponders.

Sound speed in ocean can be directly measured by lowering and hoisting a conductivity-temperature-depth profiler (CTD) overside the research vessel. However, CTD profiling and acoustic ranging are the exclusive operations in our survey style that uses a towed buoy as a surface platform. The alternative solution to achieve the simultaneous measurement is just casting an expendable CTD (XCTD) or expendable bathythermograph (XBT) into the seawater, which is less precise but much efficient and is most prevalent among oceanographers. It is worth comparing thus measured sound speed with the acoustically estimated quantity addressed above through a proper translation to be an equivalent quantity to each other. In this paper, we will present a general expression of sound speed variation in the acoustic ranging and demonstrate the degree of the agreement between the acoustically estimated sound speed and the *in situ* measurements in the framework of the proposed expression.

2. A Generalized Expression of Sound Speed

It is impractical or almost impossible to monitor temporally and spatially varying sound speed in ocean by *in situ* measurements. Spiess (1985) pointed out that "horizontal"

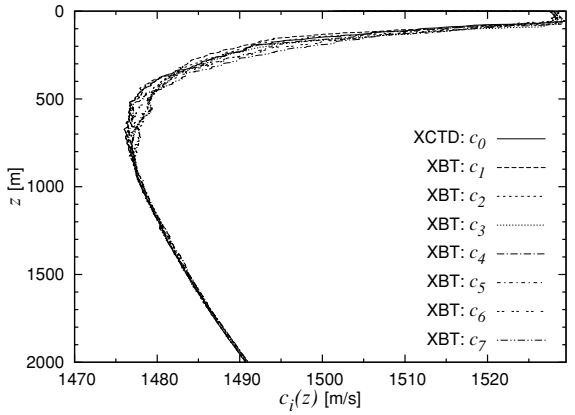

Fig. 1. Sound velocity profiles obtained by a XCTD (down to 1975 m) and seven XBT measurements (down to 1745 m). Temperature in the XBT measurements were converted into velocity using Del Grosso's empirical equation. Each temperature profile is linearly extrapolated to 2000 m so that its gradient being continuous. Fall-rates of the XBT and XCTD are corrected according to Table 1. For details, see in the text.

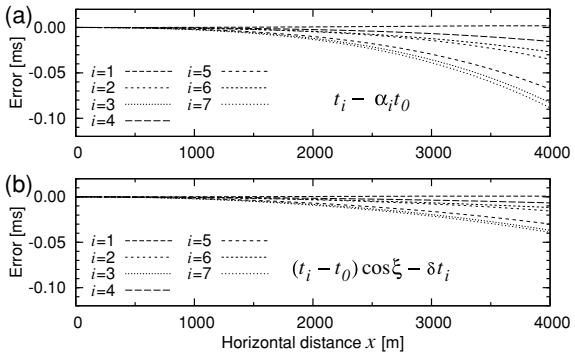

Fig. 2. Error in the synthetic two-way traveltimes to the exact solution as a function of horizontal distance (0–4000 m) with a fixed depth (2000 m) for the two different parameterization in sound speed, (a) the ratio α and (b) the residual δt. Cases for the seven XBT-inferred sound speeds ($i = 1, ..., 7$) in Fig. 1 are shown.

positioning of a transponder array is not affected by temporal variation in sound speed when acoustic ranging is made at the center of the transponder array as far as sound speed keeps stratified structure. In this case, sound speed variation is purely projected on to the apparent array depth. Employing vertically normalized traveltime residuals, the detail of which will be described later, Kido *et al.* (2006) extended this advantage even for the observed position significantly distant from the center of the array. In any case, sound speed variation is implicitly estimated as the variation in depth of the array or traveltime residuals. On the contrary, Fujita *et al.* (2006) and Sugimoto *et al.* (2006) determined individual transponder positions rather than that of the array by moving surveys and hence explicitly estimated sound speed variation.

In GPS/acoustic analysis, sound speed at a certain time can be solved only as a single quantity because the number of ranging paths at the moment is limited to the number of transponders. The quantity should be a form of integrated sound speed along the ray-path. In the case of horizontally stratified sound speed structure, the quantity can be regarded as a common value among ray-paths to different transponders on seafloor. Here we describe two different expressions of the quantity, though we employ the latter expression for further analysis.

2.1 Representing sound speed by α

The most straightforward expression of the quantity for a slowness profile $s(z)$ is α, the ratio of the traveltime of a vertical path to that for the reference profile $s_0(z)$:

$$\alpha = \int_0^Z s(z)\mathrm{d}z \Big/ \int_0^Z s_0(z)\mathrm{d}z\,, \tag{1}$$

where slowness is defined as a reciprocal of velocity ($s(z) = c^{-1}(z)$) at each depth of z down to the seafloor ($z = Z$).

Figure 1 shows sound velocity profiles $c_i(z)$ ($i = 0, ..., 7$) obtained by periodically repeated XBT measurements through the 2-day-long stationary survey at a fixed site in Kumano-nada in 2004 (Kido *et al.*, 2006). Let $c_0(z)$ be a reference profile and hence $s_0(z)$ be the reference slowness. α_i for i-th profile can be calculated by Eq. (1). Exact two-way traveltime t_i of a slant path between the surface ($z = 0$) and the seafloor ($z = Z$) is a function of the slowness profile $s_i(z)$, horizontal distance x, and Z:

$$t_i = 2 \times t(s_i(z), x, Z)\,, \tag{2}$$

which can be calculated through the ray theory within stratified media (e.g., Udías, 2000). Here we examine how the single quantity α_i provides good approximation on traveltimes for ray-paths with variable slant distances by calculating the difference between the exact and approximated traveltimes (Fig. 2(a)),

$$t_i - \alpha_i t_0\,. \tag{3}$$

$t_i - \alpha_i t_0 = 0$ at $x = 0$ since the definition in Eq. (1) is the exact solution for the vertical path. Within the possible range of all the slowness variation during the survey, the difference does not exceed 0.02 ms (=1.5 cm in slant distance) unless $x > 2000$ m, which is smaller than the precision required in the current seafloor geodesy. Therefore the expression with the simple ratio α is adequate for representing sound speed variation.

However, this approximation is valid only for flat seafloor. This is because the two slowness profiles are almost equal for greater depth as shown in Fig. 1 while Eq. (3) regards the two uniformly differ by the factor of α_i for all the depth range ($s_i(z) = \alpha_i s_0(z)$). Then α_i must be corrected by Z_k/Z_0 when Z_k, the depth of k-th transponder, is different from Z_0, the depth just underneath the buoy.

2.2 Representing sound speed by δt

On the contrary to the ratio α, we propose a difference or residual quantity to represent sound speed relative to the reference as follow:

$$\delta t = 2\int_0^Z s(z)\mathrm{d}z - 2\int_0^Z s_0(z)\mathrm{d}z = 2\int_0^Z [s(z) - s_0(z)]\,\mathrm{d}z\,. \tag{4}$$

It is obvious that exact traveltimes t_i and t_0 defined in Eq. (2) are nearly proportional to the slant distance so that their

difference $t_i - t_0$ is also proportional to the slant distance. Therefore applying the normalization with the slant distance by way of the slant angle, $\cos\xi = Z/\sqrt{x^2 + Z^2}$, we obtain a quantity $(t_i - t_0)\cos\xi$, which is nearly constant and close to δt_i.

As in the same way for α, the accuracy of the approximation is evaluated by differentiating the two quantity that

$$(t_i - t_0)\cos\xi - \delta t_i \tag{5}$$

and is plotted in Fig. 2(b) as a function of horizontal distance x.

$s(z) - s_0(z)$ for $z > 1000$ m is generally negligible (see Fig. 1) so that the integral in Eq. (4) can be truncated at a certain depth. This means that δt is independent with the seafloor depth Z and well suited to represent sound speed variation inferred from *in situ* measurements described in the next section. We henceforth denote the measured δt as δt_{XBT} or δt_{XCTD}.

3. XBT-inferred Sound Speed

In general, sound speed in seawater is greatly influenced by its temperature and pressure (depth), and slightly by salinity (conductivity). These parameters can be measured by a conductivity-temperature-depth profiler (CTD). However, a CTD requires a special winch on deck to lower and hoist the instrument and takes relatively long time to complete a profiling. An expendable bathythermograph (XBT) is a popular and convenient tool among oceanographers to efficiently infer sound speed profiles in ocean. It measures the temperature of seawater as a probe sinks at a known rate and sends the data back to the launching device in realtime through a thin wire. An expendable CTD (XCTD), on the other hand, measures electrical conductivity of seawater as well as temperature with much higher accuracy than XBT. However, because of the costly price of XCTD probes in return for its accuracy, the frequency of XCTD measurements is limited. In our research, XCTD is used to calibrate temperature and fall-rate of XBTs and to provide a typical salinity profile in a particular site for the computation of sound speeds using XBT-derived temperature profiles described later.

3.1 Fall-rate of XBT and XCTD

Since a XBT and XCTD probe has no pressure gauge, correspondence of measured data to depth or pressure depends on probe's fall-rate in ocean. Empirical equations of fall-rate for individual probe type have been investigated by oceanographers. The fall-rate is basically a function of shape and weight of the probe, which linearly lessens its weight with depth for losing built-in wire connected to the launcher at sea surface. This can be well approximated by the following equation:

$$z(t) = at - bt^2\,, \tag{6}$$

where $z(t)$ is the depth at the elapsed time t since the probe touched the seawater, and a and b are constants. Recently Kizu *et al.* (2005) recompiled numerous past collocated measurements of XBT and reliable CTD and proposed a new set of constants a_{K} and b_{K} listed in Table 1 for XBT T-5 model manufactured by Tsurumi Seiki, Co. Ltd. (TSK), which is our employed probe. According to this equation, we recompute the depth z_{K} of our XBT data instead of TSK's nominal depth z_{T} based on the original TSK constants a_{T} and b_{T}, also shown in Table 1, through the following procedure:

Table 1. Coefficients of the fall-rate equations, $z = at - bt^2$, for XBT-T5 and XCTD-2 models by TSK. Nominal values by TSK and calibrated value by Kizu *et al.* (2005) for XBT-T5 and by Koso *et al.* (2005) (SM2 in their paper) for XCTD-2 are shown.

Probe	Ref.	a [m/s]	b [m/s^2]
XBT-T5	TSK	6.828	0.00182
XBT-T5	Kizu	6.54071	0.0018691
XCTD-2	TSK	3.3997	0.0003
XCTD-2	Koso	3.4482	0.00031

$$z_{\mathrm{T}} = a_{\mathrm{T}}\, t - b_{\mathrm{T}}\, t^2 \tag{7}$$

$$t = \frac{a_{\mathrm{T}} - \sqrt{a_{\mathrm{T}}^2 - 4\, b_{\mathrm{T}}\, z_{\mathrm{T}}}}{2 b_{\mathrm{T}}} \tag{8}$$

$$z_{\mathrm{K}} = a_{\mathrm{K}}\, t - b_{\mathrm{K}}\, t^2\,. \tag{9}$$

The depth in the XCTD data is also corrected in the same way using the fall-rate proposed in Koso *et al.* (2005).

3.2 Temperature to sound speed conversion

As stated above, sound speed profile in sea water $c(z)$ is a function of profiles of three parameters: temperature $T(z)$, salinity $S(z)$, and hydrostatic pressure $P(z)$ as $c(z) = c(T(z), S(z), P(z))$. Much effort have been made to construct and improve the experimental equation of $c(T, S, P)$. Although Pike and Beiboer (1993) reported that the formula presented by Chen and Millero (1977), known as UNESCO's equation (Fofonoff and Millard, 1983), gives better sound speed than that by Del Grosso (1974) for relatively shallow continental shelf (<1000 m), most of the long-range field measurements support Del Grosso's formula (Dushaw *et al.*, 1993; Meinen and Watts, 1997). Therefore we employ Del Grosso's equation, reformulated by Wong and Zhu (1995) to adapt to the International Temperature Scale of 1990 (ITS-90).

$P(z)$ is obtained from z through depth-to-pressure formula presented by Leroy and Parthiot (1998), which covers 80% of the open seas with a single correction term relative to the standard ocean ("$\delta h_0(z)$" in their paper) instead of particular $T(z)$ and $S(z)$ profiles. Nevertheless the formula accounts only for geographic latitude and depth effects on the gravitational acceleration and averaged condition of the open seas, its overall accuracy is less than 8000 Pa (Leroy and Parthiot, 1998). This corresponds to 0.8 m in depth and 0.0136 m/s in sound speed ($\partial c/\partial z \sim 0.017$ s^{-1}) which is much smaller than the accuracy of XBT inferred sound speeds.

$S(z)$ is converted from conductivity through the Practical Salinity Scale (PSS-78) defined in Lewis (1980). Contribution of change in $S(z)$ to sound speed is relatively small; temporal change in $S(z)$ at any depth observed by several XCTD measurements during the entire survey period for a week was less than 0.04 psu (practical salinity unit). This will result in only 0.048 m/s of sound speed variation at most using the relation that $\partial c/\partial S \sim 1.2$ m/s. Therefore

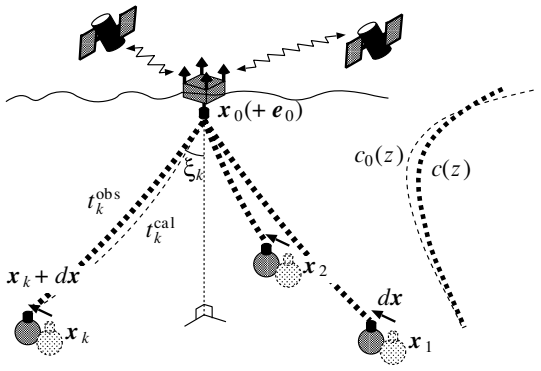

Fig. 3. An illustration of the GPS/acoustic survey using three seafloor transponders. A buoy with the transducer being kept near the array center and its position and attitude are monitored through kinematic GPS analysis of four GPS antennas on the buoy. The pre-determined position of k-th transponder, $\boldsymbol{x}_k$, is indicated with light transponders. The position to be solved, $\boldsymbol{x}_k + \delta\boldsymbol{x}$, is indicated with solid transponders. Because the analysis is performed using fixed sound speed profile, $c_0(z)$, and $\delta\boldsymbol{x}$ is limited only to horizontal displacement, t_k^{cal} is not necessary to match t_k^{obs} but δt, which is related to their difference and defined in Eq. (11), must be equal among all the transponders ($k = 1, 2, 3$). In the practical computation, $\boldsymbol{x}_0$ is separately treated as $\boldsymbol{x}_{0,\mathrm{t}}$ and $\boldsymbol{x}_{0,\mathrm{r}}$, the positions at transmission and reception of a signal.

we employ a single $S_0(z)$ obtained by a certain XCTD measurement as a representative of this particular site and period during the survey to calculate all $c_i(z)$ based on XBT-derived temperature profiles:

$$c_i(z) = c(T_i(z), S_0(z), P_i(z)), \tag{10}$$

where i is a sequential number of the XBT measurements.

4. GPS/Acoustic-inferred Sound Speed

4.1 GPS/acoustic seafloor positioning

Figure 3 illustrates the layout of our GPS/acoustic survey. A buoy with a transducer at its bottom is towed from a research vessel and is kept near the array center of the three transponders. Conducting a simultaneous acoustic ranging to the three transponders from the buoy, we can estimate $\delta\boldsymbol{x}$, the horizontal array position relative to the pre-determined array, for each ping under the assumption that the array is rigid and can move only horizontally in a stratified sound speed structure (Spiess, 1985). $\boldsymbol{x}_k$ ($k = 1, 2, 3$), the pre-determined array position and geometry, are precedently obtained by the moving survey described in Kido *et al.* (2006).

Solving the following observation equations in the analogy to Eq. (5), we obtain $\delta\boldsymbol{x}$ and δt at each time of pinging as a time-series.

$$t_k^{\mathrm{obs}} \frac{2\cos\xi_{k,\mathrm{t}}\cos\xi_{k,\mathrm{r}}}{\cos\xi_{k,\mathrm{t}} + \cos\xi_{k,\mathrm{r}}} - t_k^{\mathrm{cal}}(\boldsymbol{x}_{0,\mathrm{t}}, \boldsymbol{x}_k + \delta\boldsymbol{x}, s_0(z))\cos\xi_{k,\mathrm{t}} - t_k^{\mathrm{cal}}(\boldsymbol{x}_{0,\mathrm{r}}, \boldsymbol{x}_k + \delta\boldsymbol{x}, s_0(z))\cos\xi_{k,\mathrm{r}} - \delta t = 0 \tag{11}$$

t_k^{cal} is the synthetic one-way traveltime calculated using $c_0(z)$ for the outward and homeward travels between the transducer at a time of transmission $\boldsymbol{x}_{0,\mathrm{t}}$ or reception $\boldsymbol{x}_{0,\mathrm{r}}$ and transponder $\boldsymbol{x}_k + \delta\boldsymbol{x}$. For a stationary survey, $\xi_{k,\mathrm{t}}$ and $\xi_{k,\mathrm{r}}$ have very close value and can be regarded as their average ξ_k. The observed two-way traveltime t_k^{obs}, which is normalized by the harmonic mean of the slant ranges, must reflect the actual velocity profile, $c(z)$, and the difference from $c_0(z)$ would contribute to the vertically normalized traveltime residual, δt. We call this particular δt as δt_{Ac}. The essence of the stationary survey at the center of the array is that $\boldsymbol{x}_k$ error always reflects in $\delta\boldsymbol{x}$ error in the same way and hence has almost no effect on relative positioning or displacements among survey campaigns. Note that $\boldsymbol{x}_k$ error also contributes to δt_{Ac}, but only as a constant bias.

4.2 Error in the transducer position

Error in the transducer position $\boldsymbol{x}_0$, denoted here as $\boldsymbol{e}_0$, originates in kinematic GPS analysis itself and in uncertainty of the attitude of the buoy at the time of pinging, which is the interpolation of relatively slow sampling rate (1 Hz) of the four GPS antennas. While the horizontal components of $\boldsymbol{e}_0$ purely reflect only on $\delta\boldsymbol{x}$ estimate, the vertical component of $\boldsymbol{e}_0$, the error in the transducer depth, plays a crucial role in estimating δt. This can be examined by comparing GPS-derived transducer height to the predicted ocean tide and geoid height as shown in Fig. 4(a). The transducer height at each ping (dots) scatters $\pm$50 cm due to ocean wave, however, the difference from the prediction (thick gray line) never exceeds 10 cm after taking moving averages for 5 min (thin solid line). In general, horizontal error in the GPS analysis is smaller than the half of vertical error due to hemispherical distribution of the visible GPS satellites (Larson and Agnew, 1991). This suggests that the horizontal GPS error to be smaller than 5 cm in this survey period. Therefore $\pm$20 cm of scatter in $\delta\boldsymbol{x}$ estimate (dots in Fig. 4(b, c)) is not caused by GPS itself but mainly due to the uncertainty in the buoy attitude mentioned above and hence can be removed by taking temporal averages (solid circles with line) for its randomicity. The remaining longer time-scale undulation of $\pm$10 cm in $\delta\boldsymbol{x}$ may be caused by time varying lateral gradient of sound speed structure as described in Kido (2007).

4.3 Acoustic and XBT measured δt

Figure 4(d) demonstrates the degree of agreement between δt_{Ac} (dots) in Eq. (11) and δt_{XBT} (open circles) in Eq. (4). Note that δt_{XBT} is plotted with a bias of $+0.46$ ms to match to δt_{Ac}. The δt_{XCTD}, which is zero by definition as the reference profile, is also indicated with an open square without bias. Approximately $+0.1$ ms of difference between δt_{XCTD} and δt_{Ac} is considered as error in the pre-determined transponder positions $\boldsymbol{x}_k$, for instance by 7.5 cm shallower than the actual position or by some error in the array geometry having the equivalent contribution.

For δt_{XBT}, the plotting bias of $+0.46$ ms and above mentioned $+0.1$ ms difference, totally $+0.56$ ms, is considered as systematic error in the XBT measurements. $+0.56$ ms in the two-way δt corresponds to -0.315 m/s or -0.072°C of systematic deviation in the profile for all the depth range, which is still smaller than TSK's nominal accuracy of $\pm$0.2°C for XBT-T5 probes. Figure 5 shows the deviation of the XBT-derived temperature profiles relative to the reference XCTD profile. The largest deviation of the temperature amounts to 0.08°C even near the bottom, where temporal variation in temperature is expected to be much

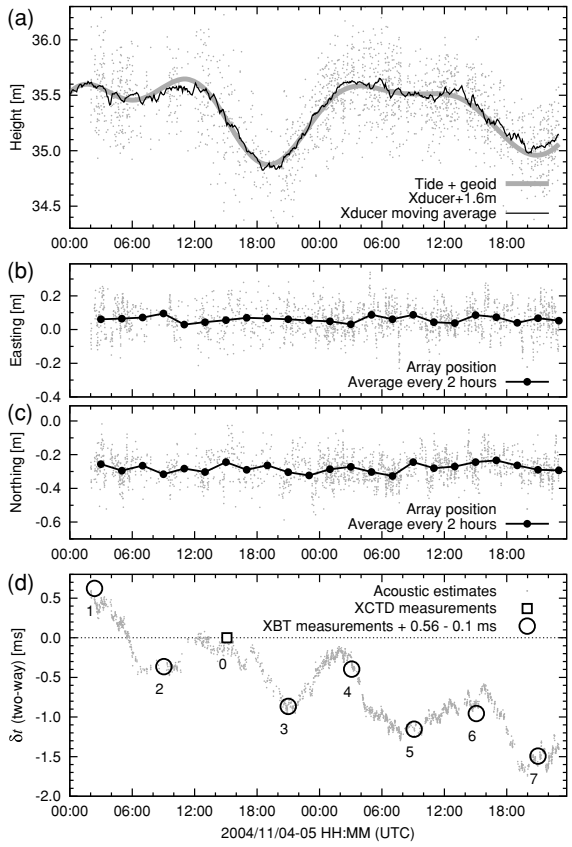

Fig. 4. Time series plots of variables during the 2-days-long survey. (a) Spheroidal height of the acoustic transducer (Xducer) equipped beneath the towed buoy (dots) at the time of each ranging ping and its 5 min. moving averages of 1 Hz height (solid line) for the removal of the scatter due to ocean waves. The values are biased by the average depth of the transducer (1.6 m) to match to the sea surface for comparison with tide. The thick gray line indicates ocean tide predicted by NAO99Jb model (Matsumoto *et al*., 2000), superimposed on the geoid height model GSIGEO2000 (Kuroishi *et al*., 2002) at this survey site. (b, c) Apparent horizontal position of the transponder array $\delta\boldsymbol{x}$ at each ping (dots) estimated through Eq. (11) and its 2-hours averages (solid circles). The easting and northing components are separately plotted. The data are identical to those shown in Kido *et al*. (2006). (d) δt_{XBT} defined by Eq. (4) obtained through seven times of XBT measurements (open circles) compared with acoustic estimate of δt_{Ac} define in Eq. (11) at each ping (dots). $\delta t_{\mathrm{XCTD}}(=0)$ for the reference velocity profile obtained by the XCTD is also indicated by a open square.

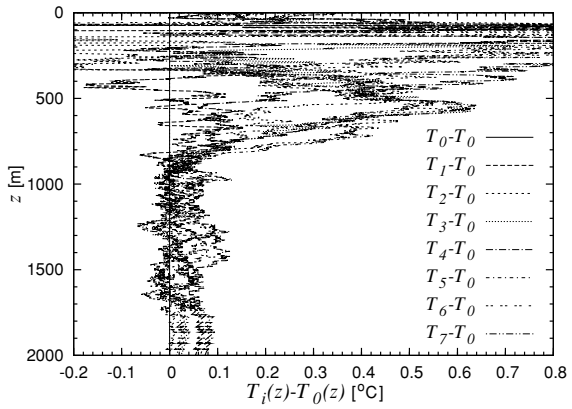

Fig. 5. Deviation of XBT-derived temperature profiles ($T_i(z)$) relative to that of XCTD ($T_0(z)$). Note that the temperature below 1745 m is linearly extrapolated.

smaller, $\sim$0.04°C, based on a few XCTD measurements during the entire cruise period (not shown here). Therefore it is highly probable that XBT-derived temperatures contain significant amount of systematic error. In addition, error in the fall-rate also results in apparent temperature deviation. It is difficult to differentiate the two effects only using the data in this study. Reseghetti *et al*. (2007) reported that XBT-derived temperatures vary 0.1°C at maximum through the numbers of collocated and contemporaneous XBT/CTD measurements. Although their XBT probes are Sippican's T4 type and differ from ours, the reported variation range is consistent with our result. They also pointed out that most XBT has positive temperature bias, which is also observed in Fig. 5. This supports applying a negative bias to temperature, hence the positive bias to δt_{XBT} to adjust to δt_{Ac}. The radius of the open circles for δt_{XBT} in Fig. 4(d) is 0.1 ms and indicates rough estimate of the maximum difference from δt_{Ac} after application of the +0.56 ms of bias. Compared to the total amplitude of temporal variation in δt_{Ac} ($\sim$2.0 ms) during the survey period, the agreement of 0.1 ms is 5% of this variation.

5. Discussions

The scatter of $\pm$0.1 ms in δt_{Ac} in Fig. 4(d) corresponds to $\pm$7.5 cm of vertical error in the transducer position, $\boldsymbol{e}_0$, which is much smaller than horizontal error of $\pm$20 cm shown in Fig. 4(b, c). This can be explained by uncertainty in the attitude of the buoy. The rolling and pitching of our buoy is relatively high frequency (typically $\sim$0.5 Hz), which leads large mis-interpolation of horizontal position of the transducer using 1 Hz data. In contrast, vertical transducer position is controlled by swells at sea-surface, which undulate slow enough to interpolate from the 1 Hz data. A high frequency GPS receiver introduced to our latest observation system would reduce these problems.

Because of the nature of the widely employed correlating technique of the pulse-compressed acoustic signal, traveltime detection is quite accurate as long as the correct peak in the correlogram is identified. In this survey, we used a step sweep signal of 8–12 kHz frequency band (20 ms in total length) with 1 MHz sampling rate. Identification of a false peak results in "cycle slip" error roughly with a 0.1 ms step. Although the step sweep signal has higher tolerance against the cycle slip error for its smaller sidelobes in correlogram, cycle slips are still observed in our current system mainly caused by following three factors: (1) Contamination of the signal due to short-range multipath in a sound-hood attached to the transducer; (2) Stretching of the signal due to Doppler's effect for the ambulant transducer; (3) Distortion of the signal due to angular dependent phase shift (Mochizuki *et al*., 2007).

When traveltimes to all the three transponders simultaneously have an error of the one cycle, their effect on δt_{Ac} is $0.1 \times \cos\xi = 0.076$ ms for our survey style that $\xi \sim 40^\circ$. In most cases, a cycle slip happens to occur for one out of the three transponders. This results in the contribution to δt_{Ac} being reduced into 1/3 and the remaining part will be

projected onto $\delta \boldsymbol{x}$ estimate. In any case, the error in the traveltime is still small compared to the accuracy in δt_{XBT}.

Sugimoto *et al*. (2006), based on their acoustic survey in the Suruga trough with repeated CTD measurements, reported that the difference between acoustically estimated and *in-situ* measured (vertically averaged) sound speed is ± 0.117 m/s in RMS and approximately ± 0.2 m/s at maximum, which is roughly 10% of amplitude of their sound speed variation itself ($\sim$2.0 m/s). This may partly due to rather hard condition in their survey field that seafloor depth is $<$900 m which is not deep enough to be stable in seawater condition beyond the lower bound of their CTD measurements. And partly due to their survey style that moves around the transponders. This is true for the result by Ishikawa and Matsumoto (2007) based on their survey at the Japan trench, where seawater condition is known to be much complicated. Horizontal gradient of sound speed structure has different contribution to traveltimes depending on slant angle, while the stationary survey keeps the same angle during the survey.

Difference of calculated sound speeds between Chen and Millero's and Del Glosso's formulae is significant. The difference increases almost linearly with depth and reaches to 0.55 m/s at 2000 m of depth, which corresponds to 0.28 ms of two-way δt. However, this will affect all the variables equally and make no noticeable change in Fig. 4(d) except for the bias.

As explained in Kido (2007), the lateral gradient of sound speed affects the apparent horizontal position of the array, but not δt estimate. In addition, the same is also true for the transducer position, in which the horizontal error is dominant due to the high frequency rolling and pitching of the buoy. Furthermore, error in the pre-determined transponder position causes a constant error as a bias in δt. These factors result in good agreement between the two independent measurements, δt_{Ac} and δt_{XBT}. This encourages the automated survey style using a moored buoy or an autonomous underwater vehicle without *in situ* sound speed measurements.

Acknowledgments. The authors thank Dr. Masashi Mochizuki for his review comments to improve the manuscript. This research is supported by DONET program, MEXT, Japan.

References

Chadwell, C. D., J. A. Hildebrand, F. N. Spiess, J. L. Morton, W. R. Normark, and C. A. Reiss, No spreading across the southern Juan de Fuca Ridge axial cleft during 1994–1996, *Geophys. Res. Lett.*, **26**, 2525–2528, 1999.

Chadwell, C. D. and F. N. Spiess, Plate motion at the ridge-transform boundary of the south Cleft segment of the Juan de Fuca Ridge from GPS-Acoustic data, *J. Geophys. Res.*, 2007 (in press).

Chadwick, W. W. and M. Stapp, A deep-sea observatory experiment using acoustic extensometers: Precise horizontal distance measurements across a mid-ocean ridge, *IEEE J. Ocean. Eng.*, **27**, 193–201, 2002.

Chen, C.-T. and F. Millero, Speed of sound in seawater at high pressure, *J. Acoust. Soc. Am.*, **62**, 1129–1135, 1977.

Del Grosso, V. A., New equation for the speed of sound in natural waters (with comparisons to other equations), *J. Acoust. Soc. Am.*, **53**, 1084–1091, 1974.

Dushaw, B. D., P. F. Worcester, and B. D. Cornuelle, On equations for the speed of sound in seawater, *J. Acoust. Soc. Am.*, **93**, 255–275, 1993.

Fofonoff, N. P. and R. C. Millard Jr., Algorithms for computation of fundamental properties of seawater, *Unesco Tech. papers in marine science*, **44**, 25–27, 1983.

Fujita, M., T. Ishikawa, M. Mochizuki, M. Sato, S. Toyama, M. Katayama, K. Kawai, Y. Matsumoto, T. Yabuki, A. Asada, and O. L. Colombo, GPS/Acoustic seafloor geodetic observation: method of data analysis and its application, *Earth Planets Space*, **58**, 265–275, 2006.

Gagnon, K., C. D. Chadwell, and E. Norabuena, Measuring the onset of locking in the Peru-Chile trench with GPS and acoustic measurements, *Nature*, **434**, 205–208, 2005.

Ishikawa, T. and Y. Matsumoto, Handling of sound speed in seafloor geodetic observation, *Tech. Bull. Hydrogr. Oceanogr.*, **25**, 100–106, 2007 (in Japanese).

Kido, M., Detecting horizontal gradient of sound speed in ocean, *Earth Planets Space*, **59**, e33–e36, 2007.

Kido, M., H. Fujimoto, S. Miura, Y. Osada, K. Tsuka, and T. Tabei, Seafloor displacement at Kumano-nada caused by the 2004 off Kii Peninsula earthquakes, detected through repeated GPS/Acoustic surveys, *Earth Planets Space*, **58**, 911–915, 2006.

Kizu, S., H. Yoritaka, and K. Hanawa, A new fall-rate equation for T-5 expendable bathythermograph (XBT) by TSK, *J. Oceanogr.*, **61**, 115–121, 2005.

Koso, Y., H. Ishii, M. Fujita, and H. Kato, An examination of the depth conversion formula of XCTD-2F, *Tech. Bull. Hydrogr. Oceanogr.*, **23**, 93–98, 2005 (in Japanese).

Kuroishi, Y., H. Ando, and Y. Fukuda, A new hybrid geoid model for Japan, GSIGEO2000, *J. Geod.*, **76**, 428–436, 2002.

Larson, K. M. and D. C. Agnew, Application of the Global Positioning System to crustal deformation measurement. I—Precision and accuracy, *J. Geophys. Res.*, **96**, 16547–16565, 1991.

Leroy, C. C. and F. Parthiot, Depth-pressure relationships in the oceans and seas, *J. Acoust. Soc. Am.*, **103**, 1346–1352, 1998.

Lewis, E. L., The practical salinity scale 1978 and its antecedents, *IEEE J. Ocean. Eng.*, **5**, 3–8, 1980.

Matsumoto, K., T. Takanezawa, and M. Ooe, Ocean tide models developed by assimilating TOPEX/POSEIDON altimeter data into hydrodynamical model: a global model and a regional model around Japan, *J. Oceanogr.*, **56**, 567–581, 2000.

Matsumoto, Y., M. Fujita, T. Ishikawa, M. Mochizuki, T. Yabuki, and A. Asada, Undersea co-seismic crustal movements associated with the 2005 Off Miyagi Prefecture Earthquake detected by GPS/acoustic seafloor geodetic observation, *Earth Planets Space*, **58**, 1573–1576, 2006.

Meinen, C. S. and D. R. Watts, Further evidence that the sound-speed algorithm of Del Grosso is more accurate than that of Chen and Millero, *J. Acoust. Soc. Am.*, **102**, 2058–2062, 1997.

Mochizuki, M., Y. Narita, T. Ishikawa, Z. Yoshida, K. Kawai, H. Matsushita, J. Kawai, H. Fuchinoue, Y. Matsumoto, M. Fujita, and A. Asada, Acoustic phase characteristics and phase centers of the acoustic transponders for seafloor geodetic observation, *Rep. Hydrogr. Oceanogr. Res.*, **43**, 29–36, 2007 (in Japanese with English abstract).

Pike, J. M. and F. L. Beiboer, A comparison between algorithms for the speed of sound in seawater, *The Hydrographic Society, Special Publication*, **34**, 1993.

Reseghetti, F., M. Borghini, and G. M. R. Manzella, Factors affecting the quality of XBT data—results of analyses on profiles from the Western Mediterranean Sea, *Ocean Sci.*, **3**, 59–75, 2007.

Spiess, F. N., Suboceanic geodetic measurements, *IEEE Trans. Geosci. Remote Sensing*, **GE 23**, 502–510, 1985.

Spiess, F. N., C. D. Chadwell, J. A. Hildebrand, L. E. Young, G. H. Purcell Jr., and H. Dragert, Precise GPS/Acoustic positioning of seafloor reference points for tectonic studies, *Phys. Earth Planet. Inter.*, **108**, 101–112, 1998.

Sugimoto, S., R. Ikuta, M. Ando, K. Tadokoro, T. Okuda, and G. M. Besana, Evaluation for GPS/Acoustic seafloor positioning based on repeated CTD measurements, *Earth Planets Space*, 2006 (submitted).

Tadokoro, K., M. Ando, R. Ikuta, T. Okuda, G. Besana, S. Sugimoto, and M. Kuno, Observation of coseismic seafloor crustal deformation due to M7 class offshore earthquakes, *Geophys. Res. Lett.*, **33**, doi: 10.1029/2006GL026742, 2006.

Udías, A., *Principles of Seismology*, pp. 490, Cambridge University Press, UK, 2000.

Wong, G. S. K. and S. Zhu, Speed of sound in seawater as a function of salinity, temperature and pressure, *J. Acoust. Soc. Am.*, **97**, 1732–1736, 1995.

M. Kido (e-mail: kido@aob.geophys.tohoku.ac.jp), Y. Osada, and H. Fujimoto